■ Molecular Dynamics | *Hot Paper* |

Reinterpretation of Dynamic Vibrational Spectroscopy to Determine the Molecular Structure and Dynamics of Ferrocene

Stephen P. Best,*[a] Feng Wang,[b] M. Tauhidul Islam,[a, c] Shawkat Islam,[b] Dominique Appadoo,[d] Ryan M. Trevorah,[c] and Christopher T. Chantler[c]

Abstract: Molecular distortion of dynamic molecules gives a clear signature in the vibrational spectra, which can be modeled to give estimates of the energy barrier and the sensitivity of the frequencies of the vibrational modes to the reaction coordinate. The reaction coordinate method (RCM) utilizes ab initio-calculated spectra of the molecule in its ground and transition states together with their relative energies to predict the temperature dependence of the vibrational spectra. DFT-calculated spectra of the eclipsed (D_{5h}) and staggered (D_{5d}) forms of ferrocene (Fc), and its deuterated analogue, within RCM explain the IR spectra of Fc in gas (350 K), solution (300 K), solid solution (7–300 K), and solid (7–300 K) states. In each case the D_{5h} rotamer is lowest in energy but with the barrier to interconversion between rotamers higher for solution-phase samples (ca. 6 kJ mol^{-1}) than for the gas-phase species (1–3 kJ mol^{-1}). The generality of the approach is demonstrated with application to tricarbonyl(η^4-norbornadiene)iron(0), Fe(NBD)(CO)$_3$. The temperature-dependent coalescence of the ν(CO) bands of Fe(NBD)(CO)$_3$ is well explained by the RCM without recourse to NMR-like rapid exchange. The RCM establishes a clear link between the calculated ground and transition states of dynamic molecules and the temperature-dependence of their vibrational spectra.

Introduction

The choreography of nuclear displacements associated with progression along a reaction coordinate is the molecular expression of reaction chemistry. While the energetics of the process is embodied in transition state theory, experimental elucidation of the molecular details has typically been linked to developments in ultrafast spectroscopic techniques.[1] We present a new approach which demonstrates that critical details of the reaction path can be obtained more directly from analysis of the temperature-dependent vibrational spectra of dynamic molecules. In so doing we resolve long-standing questions relating to the ground-state structure of ferrocene (Fc) in its different states of matter and show that the vibrational spectra of

dynamic molecules more generally can be interpreted using the concepts of transition state theory.

The ground-state structure of Fc has been the subject of long and ongoing debate since the first publications,[2] with an early conclusion of a high-symmetry staggered (D_{5d}) conformation[3] revised in light of the crystallography of low-temperature phases[4] and suggestions from electron diffraction[5] (ED) for the eclipsed (D_{5h}) conformation; this revision finding support from calculation.[6] However, the structural conclusions based on crystalline diffraction of the high-temperature monoclinic and low-temperature triclinic structures are complicated by the effects of static and dynamic disorder[7] and interpretation in terms of either limiting or an intermediate geometry[4c] is model-dependent. There is remarkably little direct experimental evidence giving unambiguous assignment of the stable rotameric form or, by extension, the dependence of the structure on the environment about the Fc molecule. Methods such as NMR[8] and inelastic neutron scattering (INS)[9] provide a measure of the dynamic character of Fc in the crystalline state, but do not identify the geometry of the most stable form. Evidence for a predominant D_{5h} conformation of Fc in the absence of the packing interactions of the low-temperature crystal is primarily derived from limited gas-phase ED measurements,[5] with recent XAFS measurements from frozen solutions showing small statistical preference for the eclipsed rotamer.[10] Surprisingly, prior to our recent suggestion that vibrational spectroscopy may allow structural assignment,[11] no spectroscopic diagnostic signature of the stereochemistry of Fc has been reported.

[a] Dr. S. P. Best, M. T. Islam
School of Chemistry, University of Melbourne
Parkville, Victoria, 3010 (Australia)
E-mail: spbest@unimelb.edu.au

[b] Prof. F. Wang, S. Islam
Department of Chemistry and Biotechnology
Swinburne University of Technology
Hawthorn, Melbourne, Victoria, 3122 (Australia)

[c] M. T. Islam, R. M. Trevorah, Prof. C. T. Chantler
School of Physics, University of Melbourne
Parkville, Victoria, 3010 (Australia)

[d] Dr. D. Appadoo
Australian Synchrotron, 800 Blackburn Road
Clayton, Victoria, 3168 (Australia)

⬚ Supporting information for this article and ORCID(s) for the author(s) are
available on the WWW under http://dx.doi.org/10.1002/chem.201603823.

We present the IR spectra of Fc and and its deuterated analogue, Fc-d, in the gas (350 K), solution (300 K), frozen solution (7–300 K), and microcrystalline solid (7–300 K) phases with the aims of 1) identifying the spectroscopic signature of the lowest-energy conformer and establishing whether a sample of Fc is present as a mixture of conformers; 2) understanding the impact of dynamic processes on the vibrational spectra and developing a framework for spectral prediction; 3) extracting the barrier for the dynamic process from the temperature-dependent vibrational spectra; and 4) establishing the generality of the approach by extension to the archetypal dynamic molecule of vibrational spectroscopy: tricarbonyl(η^4-norbornadiene)iron(0), Fe(NBD)(CO)$_3$.[12]

Results and Discussion

The sensitivity of the DFT-calculated IR spectra in the 450–500 cm^{-1} region to the stereochemistry of Fc can be understood in terms of the two normal modes occupying this region. The Q$_7$ mode[27] is calculated to be dominated by a translation of the Fe atom along the 5-fold axis and is comparatively insensitive to the relative conformations of the cyclopentadienyl (Cp) rings, whereas the Q$_{8,9}$ mode is dominated by a rotation of the Cp ligands about axes in their respective molecular planes (Figure 1) and will be subject to higher interligand repulsions when the Cp rings have an eclipsed conformation. Consequently $\Delta\nu_{7:8,9}$ ($\nu_{8,9}-\nu_7$) is significantly different for the D_{5h} (17.5 cm^{-1}) and D_{5d} (−1.8 cm^{-1}) rotamers.[11] For both rotamers the relative intensities of the bands due to the Q$_7$ and Q$_{8,9}$ modes are calculated to have an approximate 1:2 ratio and this provides a basis for assignment of the respective modes. The relative wavenumbers of ν_7 and $\nu_{8,9}$ provide a basis for identification of the stereochemistry of Fc.

The reliability of calculations of low-frequency, large amplitude, normal modes such as Q$_7$ and Q$_{8,9}$ will depend on the quality of the potential energy (PE) surface for different short and long-range interatomic interactions and would be expected to show basis-set and method dependence. The reliability of structural assignment based on DFT-calculated spectra of these modes is assessed with reference to the IR spectra of Fc in its different states of matter (Figure 1). It is immediately obvious that the spectra in this region have a band profile that is sensitive to the state of matter and, therefore, to the intra- and/or inter-molecular interactions. It is also obvious that for gas and crystalline forms of Fc the DFT-calculated IR spectra of the limiting conformers (computed for the gas-phase or solvated molecule at 0 K; Supporting Information, Table S1) bear no clear relationship to the observed spectra in terms of peak separation or relative intensity. More seriously, for the gas-phase species the relative intensities of the component bands appear to be reversed for Fc and Fc-d and inconsistent with the solution spectra (Figure 1). In contrast, the solution spectra have a band profile that could be interpreted as matching that calculated for a predominant D_{5h} isomeric form. Further, the observed and calculated ratio of ν_H/ν_D for the Q$_7$ (1.07$_{obs}$, 1.06$_{calc}$) and Q$_{8,9}$ (1.03$_{obs}$, 1.02$_{calc}$) modes of CCl$_4$ solvated Fc indicate that the calculated hydrogen atom displacement for the re-
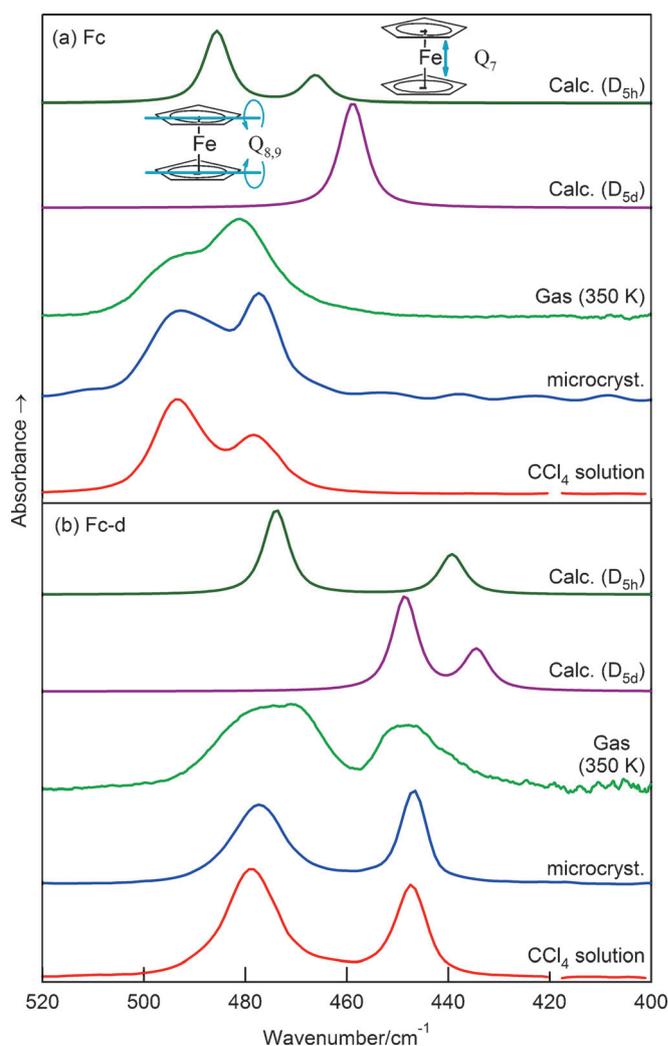

Figure 1. IR spectra of a) Fc and b) Fc-d. The DFT-calculated spectra are for the CCl$_4$-solvated molecule and are drawn with a symmetric band profile with 6 cm^{-1} FWHM. Experimental spectra were obtained at ca. 300 K (condensed phases) or 350 K (gas phase). Microcrystalline samples were prepared as KBr discs. The Q$_7$ and Q$_{8,9}$ modes are shown for D_{5h} Fc.

spective normal modes are in good agreement with experiment.[10c, 11] However, deconvolution of band profile into symmetric functions require more than the two symmetric components expected for a single rotameric form and the additional bands do not give a self-consistent set of bands in the spectrum of Fc-d. The relationship between the band profile for the Q$_7$ and Q$_{8,9}$ modes and the stereochemistry of Fc in its different phases appears far more complex than can be obtained through weighted summation of the spectra of the limiting D_{5h} and D_{5d} rotamers, and far more complex than could be represented with any sum of two symmetric band profiles.

In contrast to the sensitivity of the spectra to the phase of the sample, similar Q$_7$, Q$_{8,9}$ band profiles are obtained for solutions of Fc in CCl$_4$ and solvents with a wide range of polarity (0 to 3.92 D) which suggests a similar rotameric form. Since consideration of the motion associated with Q$_{8,9}$ lead to the expected order $\nu_{8,9}$ (D_{5h}) > $\nu_{8,9}$ (D_{5d}), identification of the stable form of Fc in solution can be established if the bands due to

both limiting rotameric forms are assigned. This is most reliably established with reference to spectra recorded at temperatures sufficiently low as to only include the most stable form of the complex. The low barrier for interconversion between the rotameric forms of Fc[8b, 13] dictates that measurements be conducted over a temperature range extending to 10 K and necessarily require study of frozen solutions. At low concentration Fc dissolves in paraffin (MP 55 °C) to give samples that are solid at RT but have IR spectra that closely match that of Fc solutions in hexane (Supporting Information, Figure S1). Moreover, the IR spectra of solid solutions of Fc and Fc-d in paraffin at 7 K (Figure 2) have $\Delta\nu_{7:8,9}$ and the relative intensities of the Q_7 and $Q_{8,9}$ bands in close agreement with that observed for the low-temperature Ar matrix-isolated forms.[14]
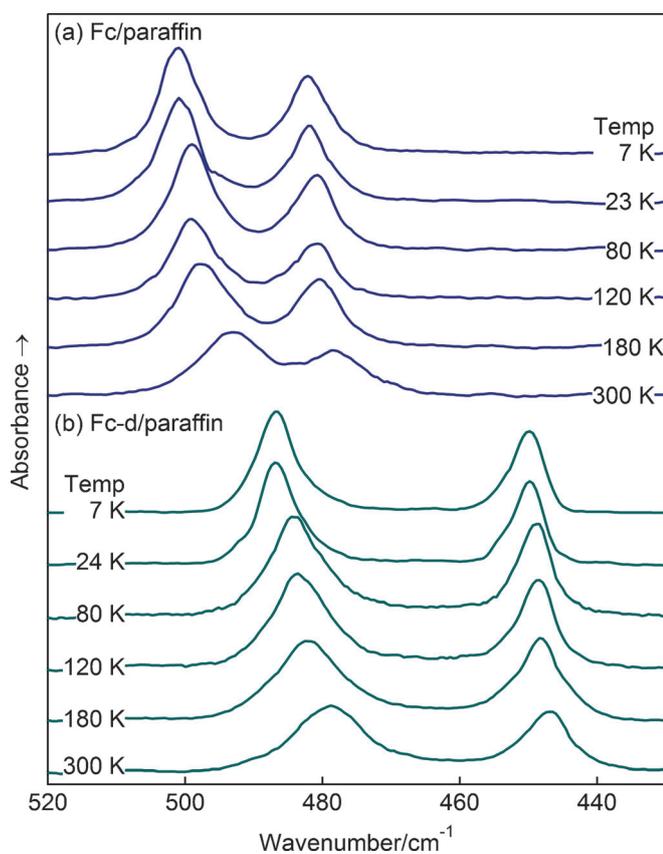

Figure 2. Temperature-dependent IR spectra of a) Fc and b) Fc-d as dilute frozen solutions in paraffin. The lower intensity, lower-wavenumber band is assigned to Q_7 and the higher-wavenumber band assigned to $Q_{8,9}$.

The temperature-dependent IR spectra of frozen solutions of Fc and Fc-d in paraffin near 480 cm^{-1} show a more intense higher-wavenumber band assigned to $Q_{8,9}$ and a lower-wavenumber band assigned to Q_7 (Figure 2). At the lowest temperatures the experimental value of $\Delta\nu_{7:8,9}$ for Fc (7 K, 18.8 cm^{-1}) is in good agreement with that calculated for the D_{5h} rotamer (19.4 cm^{-1} from DFT calculations of the CCl$_4$-solvated molecule), and for both Q_7 and $Q_{8,9}$ there is excellent agreement between the observed and calculated shifts on deuteration.

The temperature dependence of the IR spectra appear to be marked by a broadening of the Q_7 and $Q_{8,9}$ bands without the apparent growth of additional bands into the spectrum (Figure 2). Interpretation of the spectra in terms of unresolved bands due to a minority isomer is not straightforward, either the DFT calculated band profile in the Q_7, $Q_{8,9}$ region provides insufficient information to yield a reliable diagnostic signature of the rotameric forms or the reaction coordinate does not involve a well-defined intermediate. We now explore the second of these alternatives.

Vibrational spectroscopy of molecules with a low-energy barrier between isomeric forms: The reaction coordinate method (RCM)

Interconversion between D_{5h} rotamers of Fc through a D_{5d} transition state would be described by transition state theory in terms of a reaction coordinate corresponding to the relative rotation of the Cp rings about the 5-fold axis, ϕ (Figure 3). The force constant of the corresponding normal mode is related to the shape of the PE surface at the equilibrium geometry, which in turn is related to the barrier for reaction, ΔE, this being the energy difference between the D_{5h} and D_{5d} forms of Fc. The DFT-calculated lowest wavenumber vibrational mode of Fc (Q_1) has $\nu_1 = 17.3$ cm^{-1} for D_{5h} gas-phase Fc and has calculated atom displacements corresponding to the reaction coordinate. For the D_{5d} rotamer the calculation converges to a transition state 2.4 kJ mol^{-1} higher in energy with a single imaginary frequency (-29.9 cm^{-1}).[15] Taken together this allows construction of a PE surface for interconversion between rotamers (Figure 3). The shape of the PE surface is compatible with that
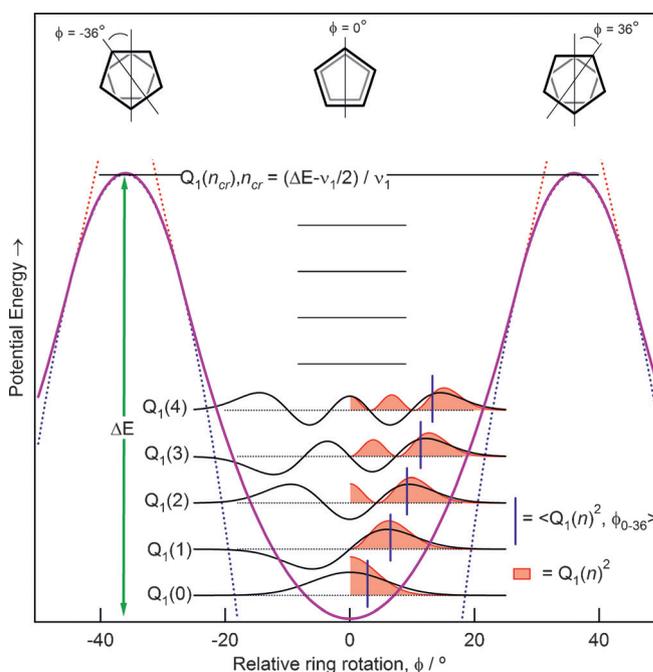
Figure 3. Representation of the potential energy surface along the Q_1 normal coordinate. Harmonic oscillator wavefunctions, their square, and $\langle Q_1(n)^2, \phi_{0-36} \rangle$ are shown for the lowest levels of Q_1.

obtained from single-point DFT calculations at points along the reaction coordinate.[16] Since Q_2 has a much higher vibrational wavenumber (167 cm^{-1}), the temperature dependence of the spectra can, in the absence of environmental effects, be understood in terms of the thermal population of the vibrational levels within the Q_1 manifold. The reaction coordinate method (RCM) assumes that the temperature dependence of the spectra can be interpreted in terms of population of the vibrational levels along the reaction coordinate.

We begin with some basic physics for any bound potential; that is, the quantum harmonic oscillator. While the wavefunctions for the vibrational levels within Q_1, $Q_1(n)$, are symmetric or antisymmetric in terms of ϕ, the molecular distortion associated with the $Q_1(n)$ levels will depend on the unsigned displacement of ϕ from zero. The time-averaged displacement for the vibrational levels is given by the expectation value of $\psi(Q_1(n))^2$, $\langle Q_1(n)^2 \rangle$, evaluated for $\phi=0$ to 36°. It is immediately clear that $\langle Q_1(0)^2, \phi_{0-36} \rangle$ has a non-zero value of ϕ, where consideration of harmonic oscillator wavefunctions suggest $\langle Q_1(0)^2, \phi_{0-36} \rangle \approx 2.8°$, with this value increasing with higher vibrational levels (Figure 3). Similar considerations apply for the vibrational level of Q_1 at the crossing of the PE surfaces, n_{cr}. For simplicity we idealize that the difference between $\langle Q_1(0)^2, \phi_{0-36} \rangle$ and $\langle Q_1(n_{cr})^2, \phi_{0-36} \rangle$ to be 75% of 36° (for a flat potential and a uniform distribution the maximum possible is 50%) and approximate a linear interpolation of the $\langle Q_1(n), \phi_{0-36} \rangle$ values from $n=0$ to n_{cr}. Neglecting anharmonicity, n_{cr} and $\langle Q_1(n)^2, \phi_{0-36} \rangle$ are given by:

$$n_{cr} = \Delta E / \nu_1 - \tfrac{1}{2} \quad (1)$$

$$\langle Q_1(n)^2, \phi_{0-36} \rangle = \langle Q_1(0)^2, \phi_{0-36} \rangle + n \langle \Delta Q_1 \rangle / n_{cr} \quad (2)$$

where $\langle Q_1(0)^2, \phi_{0-36} \rangle = 2.8°$ and $\langle \Delta Q_1 \rangle = 27°$.

The impact of population of the different vibrational levels of Q_1 will be propagated into the higher-wavenumber normal modes through the change in average value of ϕ. The DFT calculations provide the vibrational frequencies of the molecule in the D_{5h} and D_{5d} forms; that is, for ϕ equal to 0° and 36°. If it is assumed that there is a linear dependence of the wavenumber of the normal mode and ϕ then the wavenumbers of the normal modes for population of the different $Q_1(n)$ levels is given by Eq. (3):

$$\nu_y(n) = \nu_y(D_{5h}) + \langle Q_1(n)^2, \phi_{0-36} \rangle \cdot \Delta\nu_y / 36 \quad (3)$$

where $\Delta\nu_y = \nu_y(D_{5d}) - \nu_y(D_{5h})$.

Two important consequences follow from these considerations: first, that the wavenumbers of the vibrations at the equilibrium D_{5h} geometry do not correspond to the expected wavenumber of the normal modes, and more significantly, the temperature dependence of the bands in the vibrational spectra is directly interpretable in terms of the reaction coordinate. Since Q_7 and $Q_{8,9}$ of Fc have a significantly different sensitivity to ϕ, the band profile predictions will be strongly temperature-dependent.

The RCM-calculated spectra of Fc at any temperature can be generated using the energy difference between the D_{5h} and D_{5d} conformers, the calculated IR spectra (wavenumbers and intensities), and, to minimize parameterization, a single band profile for the individual $Q_y(n)$ components. The relative intensities of the $Q_y(n)$ component bands is based on the Boltzmann population of the $Q_1(n)$ levels.

Application of the RCM to the IR spectra of Fc

The RCM-calculated Q_7, $Q_{8,9}$ band profile for Fc and Fc-d for the gas-phase species at 350 K are shown in Figure 4. The full width at half maximum (FWHM) of the Gaussian/Lorentzian band profile was set to 6 cm^{-1} for both Fc and Fc-d, and calculated wavenumbers, intensities, and reaction coordinate are obtained from the DFT calculations without scaling. Aside from a modest 14 cm^{-1} offset in the calculated band wavenumbers, there is remarkable agreement between the calculated and observed spectra, a conclusion obscured by consideration only of the calculated spectra of the D_{5h} and D_{5d} forms (Figure 4 a,b).
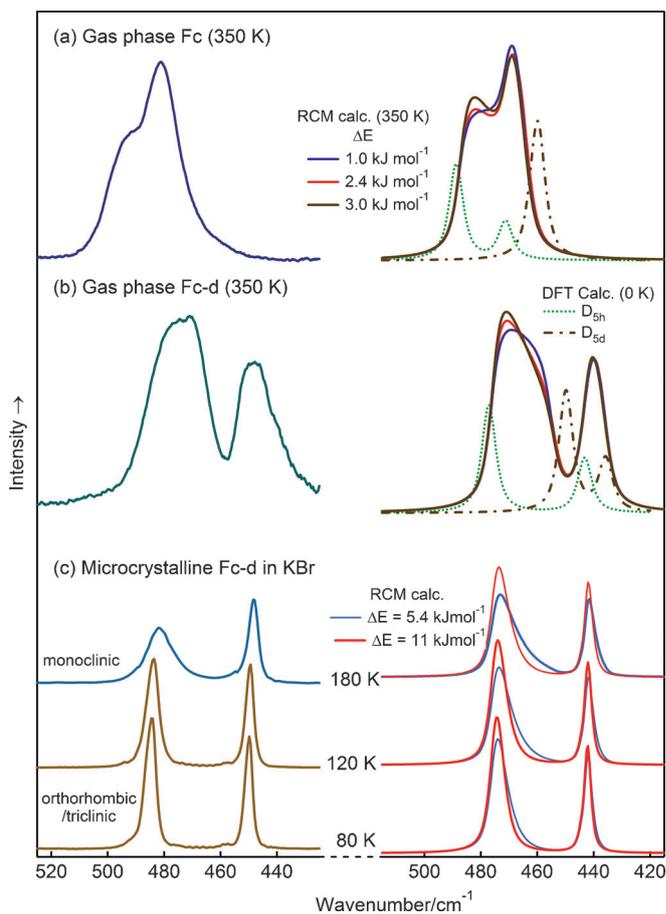
Figure 4. Experimental and calculated IR spectra of gas-phase spectra of a) Fc and b) Fc-d and c) microcrystalline Fc-d in KBr. RCM-calculated spectra were obtained using the DFT calculated values of ν_1 and ν_7, I(Q_7), $\nu_{8,9}$, and I($Q_{8,9}$) of D_{5h} and ν_7 and $\nu_{8,9}$ of D_{5d} gas-phase Fc/Fc-d (shown). For gas-phase spectra, a FWHM of 6 cm^{-1} was used for all component bands. For the microcrystalline sample the FWHM of ν_7 and $\nu_{8,9}$ were set to 2.5 and 5 cm^{-1}, respectively. Other parameters (temperature, ΔE) are as indicated.

Even without addressing the simplifications made to facilitate implementation of the RCM it is clear that 1) the D_{5h} conformer of Fc is lowest in energy and this conclusion is based both on the calculated band wavenumbers and the sensitivity of the normal modes to distortion along the reaction coordinate; and 2) the D_{5d} rotamer is either a transition state or lies in a shallow well along the reaction coordinate. The available spectra are consistent with a ΔE value in the range 1–3 kJ mol^{-1} (Figure 4 a,b). There are deviations between the observed and calculated spectra, most evident in the profile of the $Q_{8,9}$ band of Fc-d. Deviations of this sort may be expected and may reflect: 1) significant (ca. 30%) population of $Q_2(1)$ at 350 K, an out of phase rocking mode of the Cp rings; 2) anharmonicity associated with the levels close to $Q_1(n_{cr})$; and 3) differences in the calculated wavenumbers and intensities of the normal modes of the D_{5h} and D_{5d} rotamers of Fc.

The Q_7, $Q_{8,9}$ band profile for the different polymorphs of crystalline Fc has recently been modeled empirically using calculated spectra of Fc with an arbitrary range of ϕ values.[14b] However, this approach does not take into account the dynamics of the system so neither allows prediction of temperature dependence of the spectra nor distinguishes between static and dynamic disorder. An independent estimate of the barrier for Cp ring rotation of Fc is available from the interpreted results of the T_1 relaxation times for the ^{1}H resonances of the solid-state NMR spectra of the high-temperature monoclinic ($>$169 K, $\Delta E = 5.4$ kJ mol^{-1}) and low-temperature phase ($<$169 K, $\Delta E \approx 11$ kJ mol^{-1}, triclinic and ca. 25 kJ mol^{-1} orthorhombic) phases.[8b] INS, incoherent quasi-elastic neutron scattering (iQENS) measurements provide mixed supporting evidence of the barriers deduced from NMR measurements and report an estimate of ν_1 for the low-temperature, triclinic phase of Fc (ca. 25 cm^{-1}).[9a] The temperature dependence of the vibrational spectra of microcrystalline Fc-d at temperatures just above and below the monoclinic to triclinic phase transition are shown in Figure 4 c together with the RCM-calculated spectra with ΔE values of 5.4 and 11 kJ mol^{-1}. The corresponding spectra of Fc are given in the Supporting Information, Figure S2. At temperatures just above the monoclinic/triclinic phase transition (ca. 160 K) the band profile in the Q_7, $Q_{8,9}$ region match the RCM calculations with ΔE set to 5.4 kJ mol^{-1}. Below the phase transition a barrier of 11 kJ mol^{-1}, or higher, give a closer representation of the spectra (Figure 4 c) and one fully consistent with the interpretation of the dynamic behavior of Fc deduced by NMR and INS measurements. It is surprising that the dynamic behavior of Fc has a greater impact on the vibrational spectra of crystalline Fc than the effects of a change in site group symmetry and factor group coupling and presents new opportunities for the identification and study of dynamic processes in crystalline environments.

Consideration of the Q_7, $Q_{8,9}$ band profile for solutions/frozen solutions of Fc at 300 K suggests a value of ΔE higher than that of the monoclinic phase (Figure 1 and Figure 2). An increase of ΔE to 6 kJ mol^{-1} with ν_1 set to the value used for crystalline Fc, 25 cm^{-1}, and band parameters for Q_7 and $Q_{8,9}$ from the gas-phase calculations yields calculated band profiles of Fc and Fc-d for solutions and frozen solutions qualitatively

in good agreement with experiment (Figure 1, Figure 2, and Figure 5). The spectra for Fc-d were calculated by applying the calculated isotopic shifts to the respective vibrational frequencies. At temperatures below that needed to give significant population of $Q_2(1)$ (7–180 K), the asymmetry of the band profile of the experimental spectra is remarkably well-matched by the RCM calculation (Figure 2 and Figure 5). This indicates that the calculations accurately reproduce the sensitivity of the Q_7 and $Q_{8,9}$ modes to the reaction coordinate and, since the calculated profile depends on both $\nu_{8,9}$ (D_{5h}) and $\nu_{8,9}$ (D_{5d}), provides unambiguous assignment of the stereochemistry of Fc in solution, an estimation of the barrier to rotation of the Cp ring, ΔE, and the impact of solvation on ΔE.

RCM allows self-consistent interpretation of the temperature-dependent gas, solution, frozen solution and solid-state spectra of Fc and Fc-d in the Q_7, $Q_{8,9}$ region (Figure 4 and Figure 5). In essence, the normal modes sensitive to distortion of the molecule along the reaction coordinate will have a temperature dependent band profile where population of higher vibrational levels of the reaction coordinate result in an aver-
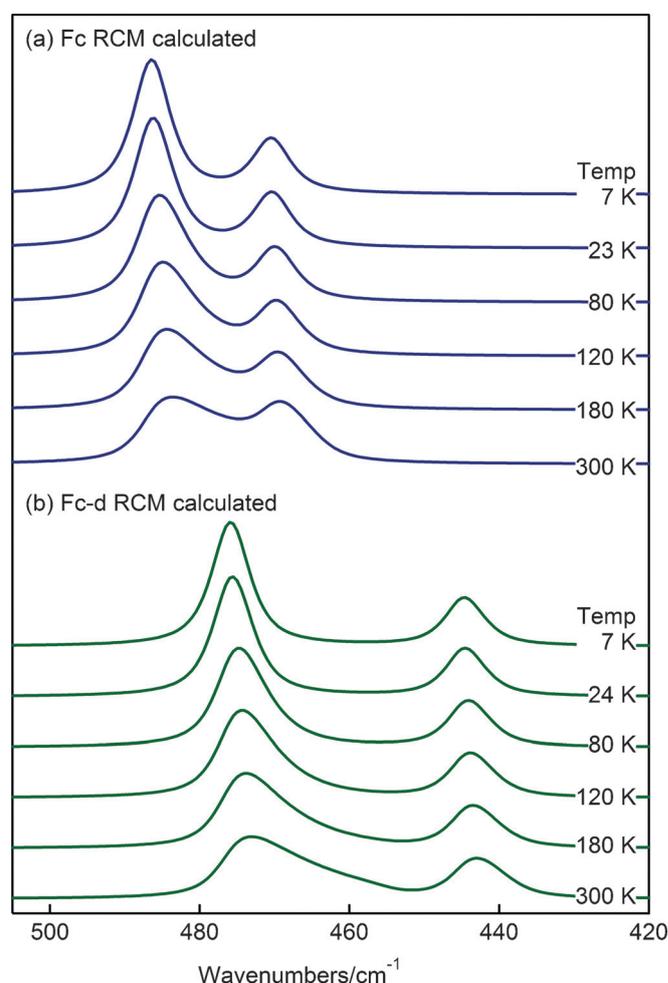
Figure 5. Temperature dependence of the RCM-calculated IR spectra of a) Fc and b) Fc-d using the gas-phase DFT calculated wavenumbers and intensities of Q_7 and $Q_{8,9}$ of the D_{5h} and D_{5d} forms of Fc. Spectra of Fc-d were calculated by applying the ν_H/ν_D calculated for the respective normal modes. Values of ΔE and ν_1 were set to 6 kJ mol^{-1} and 25 cm^{-1}, respectively.

aged geometry increasingly distorted toward the transition state. For Fc the effect of this distortion can be deduced from the DFT calculated vibrational spectra of the D_{5h} and D_{5d} rotamers. These investigations demonstrate that the implementation of the concepts of transition state theory, within RCM, is critical to the calculation of the temperature dependence of the vibrational spectra of dynamic molecules.

Dynamic vibrational spectroscopy and relationship to the RCM

The vibrational spectroscopy of dynamic molecules has largely been developed with reference to the temperature-dependent coalescence of the lower-wavenumber pair of $\nu(CO)$ bands in the IR and Raman spectra of $Fe(NBD)(CO)_3$.[17] The temperature dependence of the spectra has been modeled within a formalism based on NMR-like rapid exchange between the normal modes, where there is a different rate of exchange between the three carbonyl normal modes yielding estimates for the respective rate constants.[18] While the physical interpretation of the calculations is called into question by recent 2D-IR studies of related complexes,[19] the approach provides a means of investigating solvation effects on the molecular dynamics[18] and the measurement of the rates of electron-transfer processes.[20]

The barrier for the turnstile CO rotation of $Fe(NBD)(CO)_3$ is estimated to be ca. $6\ kJ\,mol^{-1}$,[21] similar to that for rotation of the Cp ring of Fc, and the framework for interpretation of the impact of the dynamic behavior on the vibrational spectra should be consistent for both molecules. However, explanation of the dynamic spectroscopy of $Fe(NBD)(CO)_3$ in terms of thermal population of vibrational levels of the normal mode corresponding to the turnstile CO rotation[22] was dismissed on the basis that DFT calculations "proved" that the $\nu(CO)$ modes are not sensitive to displacements corresponding to the turnstile CO rotation.[23] Such an argument would apply to the RCM. A critical point, previously overlooked, is that the similarity of the $\nu(CO)$ bands calculated for the ground and transition states of $Fe(NBD)(CO)_3$ does not require that the $\nu(CO)$ spectra are insensitive to progress of the turnstiles rotation. Indeed, both the general sensitivity of the $\nu(CO)$ spectra of $Fe(CO)_3$ complexes with related diene ligands to the orientation of the vinyl bonds and the difference in the calculated M—C and CO bond lengths for the CO ligands approximately oblique and parallel to the C=C bonds of the NBD ligand[23] argue for a sensitivity of the FeCO bonding to the orientation of the NBD ligand. This is reflected by the sensitivity of the d-orbital energies to the rotation angle of the $Fe(CO)_3$ fragment as can be shown by ligand-field calculations (Supporting Information, Figure S3). If the Fe—CO interactions of the three CO groups depend on the orientation of the NBD ligand then at orientations where the three Fe—CO interactions are similar, the $Fe(CO)_3$ fragment will have approximate C_{3v} symmetry and an A+E pair of $\nu(CO)$ bands is expected. Orientations where the Fe—CO interactions are most different will give a splitting of the doubly-degenerate E mode. It would appear as though the ground and transition state correspond to a case where there

is a similar difference in the Fe—CO interaction for the three carbonyl ligands. These considerations suggest that the calculated bands at 1971 and $1982\ cm^{-1}$ move to 1981 and $1971\ cm^{-1}$, respectively, on progression from the ground to the transition state. That is, there is an effective changeover in the order of the two lowest-wavenumber $\nu(CO)$ modes.

The published DFT-calculated $\nu(CO)$ wavenumbers of $Fe(NBD)(CO)_3$ in its ground and transition state[23] together with the experimental estimate of the barrier height, ΔE, ($6\ kJ\,mol^{-1}$)[21a, 24] allow calculation of the temperature dependence of the profile of the $\nu(CO)$ bands in the IR spectrum (Figure 6). The FWHM and intensity of the CO bands matches the lowest wavenumber spectra. Whilst a single FWHM was sufficient for modeling the temperature dependence of the broader Q_7 and $Q_{8,9}$ bands of Fc, it was necessary to increase the FWHM of the component bands for the higher temperature spectra. Since population of vibrational levels of other low
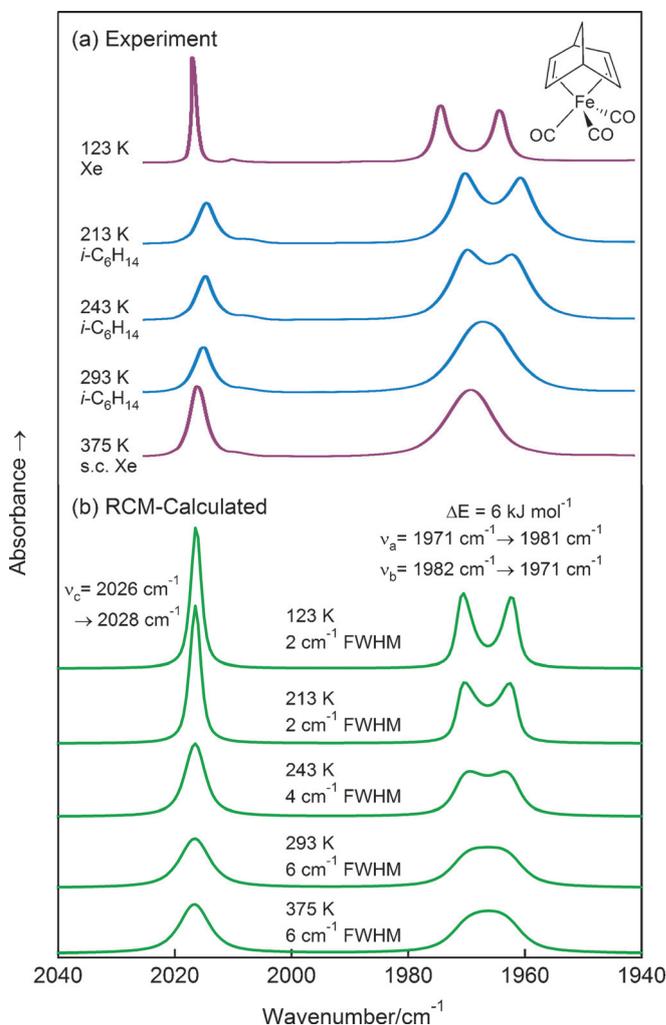
Figure 6. a) Experimental and b) RCM-Calculated IR spectra of $Fe(NBD)(CO)_3$. The calculated spectra use the DFT-calculated spectra for the ground and transition states from Ref. [23] and the experimental spectra are redrawn from the spectra presented by Turner et al.[17b] and Giodarno and Lear[18b] and were obtained either as matrix-isolated samples in Xe or as solutions in 2-methylpentane (i-C_6H_{14}) or supercritical Xe.

wavenumber normal modes increasingly impact upon the spectra, the interpretation of the high-temperature spectra requires more detailed analysis.

In the range where the temperature dependence of the spectra are dominated by population of the vibrational levels within Q_1 (below ca. 250 °C), the RCM using unmodified calculated $\nu(CO)$ band wavenumbers and experimental value of ΔE reproduce the main features of the temperature dependence of the vibrational spectra of Fe(NBD)(CO)$_3$ (Figure 6). Ironically, the calculations of Bühl and Thiel,[23] rather than dismissing Strauss' explanation[22b] of the IR spectrum of Fe(NBD)(CO)$_3$, identify the conditions where NMR-like lifetime broadening calculations can give a deceptively good representation of the band profile; that is, in cases where there is a crossover in the order of the relative wavenumbers of modes sensitive to the reaction coordinate. In contrast to NMR-like lifetime broadening, the RCM can be related directly to transition state theory in a manner consistent with conclusions drawn from 2D-IR measurements of ultrafast relaxation of Fe(cyclooctadiene)(-CO)$_3$.[19]

Conclusion

Detailed consideration of the temperature dependence of the Q_7 and $Q_{8,9}$ modes of Fc demonstrate clearly that the calculated vibrational spectra of dynamic molecules must take into account the ground and transition states and the energy difference between these forms. Simple approximations of the impact of displacements along the reaction coordinate allow implementation of the RCM and are shown to predict the temperature dependence of the spectra in remarkably close qualitative agreement with experiment. The temperature-dependent spectra of gas, solution, frozen solution, and crystalline solid forms of Fc can be explained within a self-consistent framework using the RCM. In all cases the D_{5h} rotamer is the most stable form, where assignment of the ground state structure is based on the calculated spectra of both the D_{5h} and D_{5d} forms of Fc; that is, the sensitivity of the higher wavenumber modes to distortion of the molecule along the reaction coordinate. In fact, this provides the strongest experimental evidence for the ground state conformation of Fc.

The temperature dependence of the vibrational spectra of dynamic molecules provides experimental evidence for key parameters defining the reaction coordinate. This presents a critical test of the accuracy of ab initio calculations of transition-state energy and geometry, including solvation. The DFT calculations presented in this study for the gas-phase species converged to give values of ΔE and ν_1 in excellent agreement with experiment. Extension of the calculations to include modeling the effects of solvation gives unreliable results for the low wavenumber, high amplitude vibrations, and ΔE. The comparative insensitivity of ΔE for Fc to the polarity of the solvent, for example, provides a new benchmark for assessing the predictive power of computational models of solvation.

The RCM outlined herein can be applied generally to molecules with low-energy dynamic processes, for example, Fe(NBD)(CO)$_3$, which previously were explained in terms of

non-physical NMR-like dynamic exchange of bands (modes) in the vibrational spectra. Moreover, the interpretative framework of the RCM sits comfortably with ultrafast intramolecular vibrational redistribution measured by 2D IR spectroscopy.[19] Any description of dynamic effects in the vibrational spectra must take into account the spectra of the molecule in its ground and transition states and the barrier for the dynamic process. RCM can provide the interpretative framework for testing and refinement of ab initio methods for the calculation of ground and transition-state geometry and, importantly, establishing experimental methods for charting the reaction coordinate.

Experimental Section

Commercial samples of Fc (Aldrich) and Fc-d (98.9 atom % D, CDN Isotopes) and solvents and paraffin (55 °C MP, CHEM-SUPPLY) were used as received. The sample of Fc-d has 98.9 atom % D, this corresponds to a 90:10 mixture of Fc-d$_{10}$ and Fc-d$_9$. IR spectra were obtained using either a Bruker Vertex 60 FTIR (room-temperature samples) or a Bruker IFS 125/HR interferometer FTIR coupled to the THz/Far-IR beamline at the Australian Synchrotron. Gas-phase spectra were obtained using a 60 cm multipass gas cell heated to ca. 80 °C with either a Si bolometer, Si:B photodetector, or narrow-band MCT detector. Low-temperature measurements employed a 6 K closed-loop pulse tube cryostat from Cryo Industries of America with a Lakeshore Model 336 temperature controller. Solid solutions of Fc in paraffin were prepared by dissolving a 1 % mixture of the sample in paraffin at 70–80 °C in a covered watch glass. The solution was cooled and ca. 60 mg of Fc:paraffin transferred to a 13 mm press. Teflon spacers were used to facilitate separation of the paraffin from the die pellets. For measurements having low concentrations of Fc (gas-phase and solid solutions in paraffin) the subtraction of background effects is complicated by periodic oscillations due to multiple-reflection from optical components and the sample. The periodic oscillations in the background were fitted in spectral regions close to the bands of interest and the correction applied over the full spectrum.

The density functional theory (DFT) based B3LYP functional is employed in the calculations for the eclipsed and staggered Fc, along with the recently developed basis set m6–31G(d) basis set[25] for the transition metal Fe. All quantum mechanical calculations were performed using the Gaussian 09 computational chemistry package.[26]

RCM band profiles were calculated by summing the $Q_x(n)$ contributions for the normal modes. The relative intensities of the components was obtained using a Boltzmann population and the $\nu_x(n)$ values were obtained using equations 1–3 and, unless otherwise stated, a Gaussian:Lorentzian function with a single FWHM, typically 6 cm^{-1}, was used for all component bands. IR spectra of Fc-d were calculated as a 90:10 mixture of Fc-d$_{10}$ and Fc-d$_9$ so as to match the isotopic composition of the experimental sample. The ν_H/ν_D values and relative intensities for the different normal modes were obtained from DFT calculation of the relevant isotopic species.

[1] a) T. Kobayashi, *Bull. Chem. Soc. Jpn.* **2013**, *86*, 167–182; b) M. Chergui, *Acc. Chem. Res.* **2015**, *48*, 801–808; c) J. K. McCusker, A. Vlcek Jr., *Acc. Chem. Res.* **2015**, *48*, 1207–1208.

[2] J. I. Seeman, S. Cantrill, *Nat. Chem.* **2016**, *8*, 193–200.

[3] a) E. O. Fischer, W. Pfab, *Z. Naturforsch. B* **1952**, *7*, 377–379; b) G. Wilkinson, M. Rosenblum, M. C. Whiting, R. B. Woodward, *J. Am. Chem. Soc.* **1952**, *74*, 2125–2126; c) J. D. Dunitz, L. E. Orgel, *Nature* **1953**, *171*, 121–122.

[4] a) K. Ogasahara, M. Sorai, H. Suga, *Chem. Phys. Lett.* **1979**, *68*, 457–460; b) P. Seller, J. D. Dunitz, *Acta Crystallogr. Sect. B* **1979**, *35*, 2020–2032; c) F. Takusagawa, T. F. Koetzle, *Acta Crystallogr. Sect. B* **1979**, *35*, 1074–1081; d) P. Seiler, J. D. Dunitz, *Acta Crystallogr. Sect. B* **1982**, *38*, 1741–1745.

[5] a) R. K. Bohn, A. Haaland, *J. Organomet. Chem.* **1966**, *5*, 470–476; b) A. Haaland, J. E. Nilsson, *Chem. Commun.* **1968**, 88–89.

[6] S. Coriani, A. Haaland, T. Helgaker, P. Jorgensen, *Chemphyschem* **2006**, *7*, 245–249.

[7] a) P. Seiler, J. D. Dunitz, *Acta Crystallogr. Sect. B* **1979**, *35*, 1068–1074; b) J. D. Dunitz, *Acta Crystallogr. Sect. B* **1995**, *51*, 619–631.

[8] a) A. Kubo, R. Ikeda, D. Nakamura, *J. Chem. Soc. Faraday Trans.* **1986**, *82*, 1543–1562; b) A. Kubo, R. Ikeda, D. Nakamura, *Chem. Lett.* **1981**, *10*, 1497–1500.

[9] a) M. Appel, B. Frick, T. L. Spehr, B. Stuhn, *J. Chem. Phys.* **2015**, *142*; b) E. Kemner, I. M. de Schepper, G. J. Kearley, U. A. Jayasooriya, *J. Chem. Phys.* **2000**, *112*, 10926–10929.

[10] a) M. T. Islam, S. P. Best, J. D. Bourke, L. J. Tantau, C. Q. Tran, F. Wang, C. T. Chantler, *J. Phys. Chem. C* **2016**, *120*, 9399–9418; b) J. D. Bourke, M. T. Islam, S. P. Best, C. Q. Tran, F. Wang, C. T. Chantler, *J. Phys. Chem. Lett.* **2016**, *7*, 2792–2796; c) C. T. Chantler, N. A. Rae, M. T. Islam, S. P. Best, J. Yeo, L. F. Smale, J. Hester, N. Mohammadi, F. Wang, *J. Synchrotron Radiat.* **2012**, *19*, 145–158.

[11] N. Mohammadi, A. Ganesan, C. T. Chantler, F. Wang, *J. Organomet. Chem.* **2012**, *713*, 51–59.

[12] J. J. Turner, in *Handbook of vibrational spectroscopy, Vol. 1* (Eds.: P. R. Griffiths, J. M. Chalmers), Wiley, New York, **2001**, pp. 101–127.

[13] a) A. Haaland, J. E. Nilsson, *Acta Chem. Scand.* **1968**, *22*, 2653–2670; b) A. Kubo, R. Ikeda, D. Nakamura, *J. Chem. Soc. Faraday Trans.* **1986**, *2*, 1543–1562.

[14] a) R. W. Kugel, L. F. Pinelo, B. S. Ault, *J. Phys. Chem. A* **2015**, *119*, 2371–2382; b) P. A. Silva, T. M. R. Maria, C. M. Nunes, M. E. S. Eusebio, R. Fausto, *J. Mol. Struct.* **2014**, *1078*, 90–105.

[15] S. Islam, F. Wang, *RSC Adv.* **2015**, *5*, 11933–11941.

[16] Y. Yang, L. Yu, *PhysChemChemPhys* **2013**, *15*, 2669–2683.

[17] a) A. Vlcek, Jr., *Inorg. Chem.* **1992**, *4*, 189–193; b) J. J. Turner, F. W. Grevels, S. M. Howdle, J. Jacke, M. T. Haward, W. E. Klotzbuecher, *J. Am. Chem. Soc.* **1991**, *113*, 8347–8353; c) F. W. Grevels, K. Kerpen, W. E. Klotzbucher, R. E. D. McClung, G. Russell, M. Viotte, K. Schaffner, *J. Am. Chem. Soc.* **1998**, *120*, 10423–10433.

[18] a) A. N. Giordano, B. J. Lear, *J. Phys. Chem. A* **2015**, *119*, 3545–3555; b) A. N. Giordano, B. J. Lear, *J. Phys. Chem. A* **2013**, *117*, 12313–12319.

[19] A. D. Hill, M. C. Zoerb, S. C. Nguyen, J. P. Lomont, M. A. Bowring, C. B. Harris, *J. Phys. Chem. B* **2013**, *117*, 15346–15355.

[20] C. H. Londergan, C. P. Kubiak, *Chem-Eur. J.* **2003**, *9*, 5962–5969.

[21] a) F. W. Grevels, J. Jacke, K. Seevogel, *J. Mol. Struct.* **1988**, *174*, 107–112; b) J. J. Turner, C. M. Gordon, S. M. Howdle, *J. Phys. Chem.* **1995**, *99*, 17532–17538.

[22] a) R. A. Macphail, H. L. Strauss, *J. Chem. Phys.* **1985**, *82*, 1156–1166; b) H. L. Strauss, *J. Am. Chem. Soc.* **1992**, *114*, 905–907.

[23] M. Bühl, W. Thiel, *Inorg. Chem.* **1997**, *36*, 2922–2924.

[24] F. W. Grevels, J. Jacke, W. E. Klotzbuecher, C. Krueger, K. Seevogel, Y. H. Tsay, *Angew. Chem.* **1987**, *99*, 960–961.

[25] A. V. Mitin, J. Baker, P. Pulay, *J. Chem. Phys.* **2003**, *118*, 7775–7782.

[26] M. J. Frisch, G. W. Trucks, H. B. Schlegel, G. E. Scuseria, M. A. Robb, J. R. Cheeseman, G. Scalmani, V. Barone, B. Mennucci, G. A. Petersson, H. Nakatsuji, M. Caricato, X. Li, H. P. Hratchian, A. F. Izmaylov, J. Bloino, G. Zheng, J. L. Sonnenberg, M. Hada, M. Ehara, K. Toyota, R. Fukuda, J. Hasegawa, M. Ishida, T. Nakajima, Y. Honda, O. Kitao, H. Nakai, T. Vreven, J. A. Montgomery Jr., J. E. Peralta, F. Ogliaro, M. J. Bearpark, J. Heyd, E. N. Brothers, K. N. Kudin, V. N. Staroverov, R. Kobayashi, J. Normand, K. Raghavachari, A. P. Rendell, J. C. Burant, S. S. Iyengar, J. Tomasi, M. Cossi, N. Rega, N. J. Millam, M. Klene, J. E. Knox, J. B. Cross, V. Bakken, C. Adamo, J. Jaramillo, R. Gomperts, R. E. Stratmann, O. Yazyev, A. J. Austin, R. Cammi, C. Pomelli, J. W. Ochterski, R. L. Martin, K. Morokuma, V. G. Zakrzewski, G. A. Voth, P. Salvador, J. J. Dannenberg, S. Dapprich, A. D. Daniels, Ö. Farkas, J. B. Foresman, J. V. Ortiz, J. Cioslowski, D. J. Fox, Gaussian, Inc., Wallingford, CT, USA, **2009**.

[27] The normal modes are labeled Q_x, where x is numbered according to the energy of the normal mode calculated for the D_{5h} form of Fc. For degenerate modes, multiple numbers are indicated. The wavenumbers of the fundamentals of the respective normal modes are labeled as ν_x. Transitions initiated from excited vibrational levels of Q_1 are designated $Q_x(\%)$ or $\nu_x(\%)$, where x designates the normal mode and % the vibrational level of the Q_1 normal mode.